*Electronic Supplementary Data*

# A Dual-Channel Chemodosimetric Sensor for Discrimination between Hypochlorite and nerve-agent mimic DCP: Application on Human Breast Cancer Cells

Moumi Mandal[a], Uday Narayan Guria[a], Anirban Karak[a], Satyajit Halder[b], Deepanjan Banik[a]

Kuladip Jana[b], Arik Kar[a], Ajit Kumar Mahapatra[a]*

*[a]Department of Chemistry, Indian Institute of Engineering Science and Technology, Shibpur, Howrah 711 103, India*
*[b]Division of Molecular Medicine, Bose Institute, P 1/12, CIT Scheme VIIM, Kolkata-700 054, India.*

*Author to whom correspondence should be addressed; electronic mail: akar@chem.iiests.ac.in; Tel.: +0091 8334845357

*Author to whom correspondence should be addressed; electronic mail: akmahapatra@chem.iiests.ac.in; Tel.: +91 – 9434508013

**Table of contents**

**Table S1** Comparison between the previously reported DCP sensors with our current work.

| Probe structure | Lod | Solvent | Mode of sensing | Application | Ref. |
|---|---|---|---|---|---|
|  | 10.4 nM | Acetonitrile. | Covalent assembly" and Lossen rearrangement. | TLC based test strip | 1 |
|  | 88 nM | Chloroform. | Suppresses of the PET process | Polystyrene membrane based test strip | 2 |
|  | $2.1 \times 10^{-8}$ M | $CH_3CN/H_2O$ (1 : 1, v/v) | Blocking of ICT | TLC based test strip | 3 |
|  | 33.5 nM. | DMF | Inhibition of PET and ESIPT | Nano fiber based test strip | 4 |
|  | $8.45 \times 10^{-8}$ M | THF/H2O (4/1, v/v) | Enhancement of ICT | TLC based test strip | 5 |

| Structure | LOD | Medium | Mechanism | Application | Ref |
|---|---|---|---|---|---|
|  | 0.2 μM | DCM (with 3% Et3N) | Spirolactam ring opening | TLC based test strip | 6 |
|  | 0.78 μmol/L | Methanol. | - | Polyethylene glycol (PEG) membrane-based test strips | 7 |
|  | 0.14 μM. | $CH_3CN$-$H_2O$ (10 mM HEPES buffer, 4:6 v/v, pH 7.4 at 25 °C) | Inhibition of PET | Filter paper based test strip, Cellular imaging | 8 |
|  | 0.186 μM) | $CH_3CN$ | ESIPT-OFF | Polystyrene based test strip | 9 |
|  | ($3.56 \times 10^{-8}$M | THF-H2O(8:2) | - | TLC based test strip | Our Work |
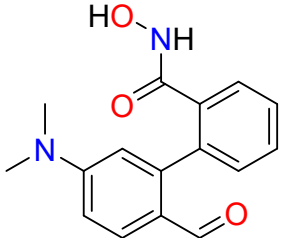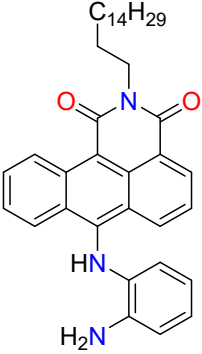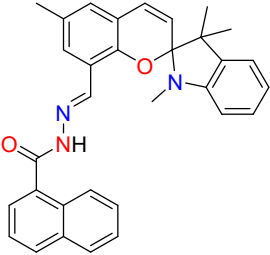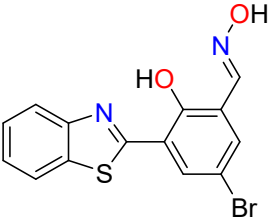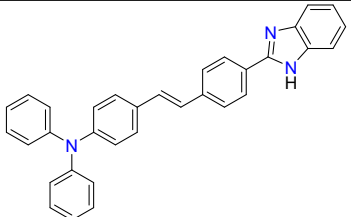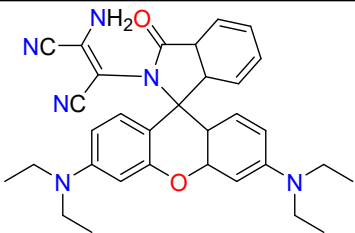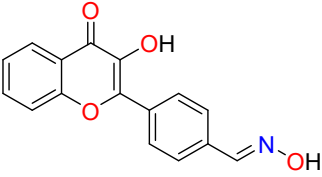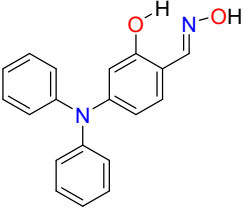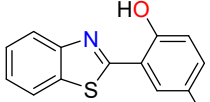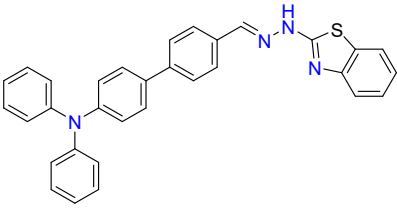
**Table S2:** Comparison between the previously reported Hypochlorite ion sensors with our current work
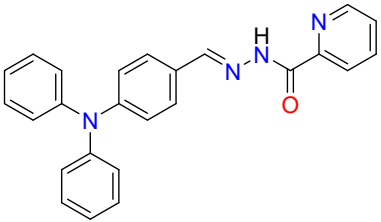
| Structure | LOD | Medium | Mechanism | Application | Ref |
|---|---|---|---|---|---|
|  | 0.8 μM. | DMSO–water solution (1: 4, v/v, 50 mM PBS buffer solution at pH 7.4). | Oxidation | Cellular imaging | 10 |
|  | $7.37 \times 10^{-7}$ M. | THF (1/1, v/v) solution | C=N isomerization | Water Test | 11 |

| Structure | Detection limit | Solvent | Mechanism | Application | Ref |
|---|---|---|---|---|---|
|  | 64.2 nM | (DMSO)/ $H_2O$ (v/v, 5 : 1) | ICT ON | Cellular imaging | 12 |
|  | 2.4 nM | PBS buffer-MeOH (v/v = 50/50, 50 mM PBS, pH 7.4) | Acid-triggered intramolecular cyclization. | Cellular imaging | 13 |
|  | 7.6 nM | PBS buffer (10 mM, 1% DMSO, pH 7.4), | Inhibition of PET | Cellular imaging | 14 |
|  | - | PBS buffer containing 50%DMF | FRET | Cellular imaging | 15 |
|  | $2.0 \times 10^{-7}$ mol/L | DMF/HEPES buffer (25:75 v/v, $1.0 \times 10^{-2}$ mol/ | Destroying the $\pi$-conjugation | Cellular imaging | 16 |
|  | $7.67 \times 10^{-8}$ M | THF-H2O(1:9) |  | Cellular imaging | Our work |
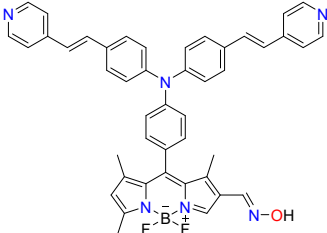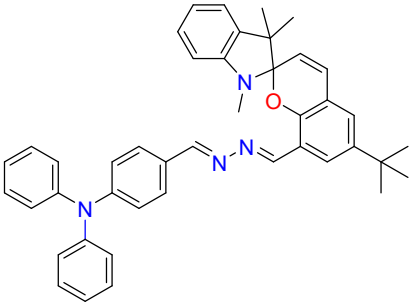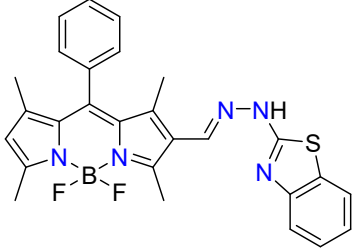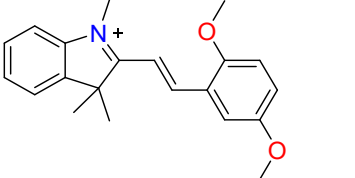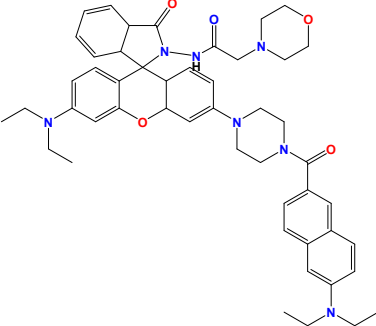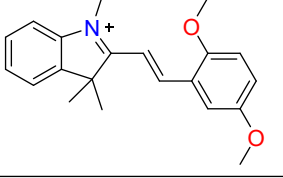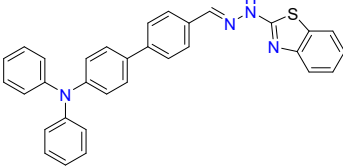
## 2. Theoretical calculations

For the determination of the electronic performance of the probe and the products which are formed after the chemodosimetric reaction with OCl⁻ and DCP, we additionally performed quantum chemical DFT calculation by using the Gaussian 09 program with the help of the Gauss View visualization program. The probes and the products have been optimized by using the B3LYP/6-311G+(d, p) basis set. The geometries are established as suitable minima by frequency calculations. Subsequently we executed the Time dependent density functional theory (TDDFT) at the identical level.
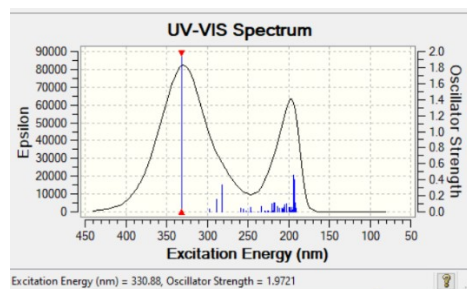


**Figure S1** Absorption spectra of the probe **TPSZ**

**Table S3.** The vertical main orbital transition of the receptor calculated by TDDFT method.

| Energy (eV) | Wavelength (nm) | Osc. strength (f) | Transition |
|---|---|---|---|
| 3.7472 | 330.88 | 1.97 | **HOMO→LUMO** |
| 4.1665 | 297.57 | 0.0300 | **HOMO→LUMO+1** |
| 4.2977 | 288.49 | 0.1555 | **HOMO-1→LUMO** |

## 3. Cellular imaging:

**Cell line study:**

To envision the fluorescence ability of the ligand **TPSA** in the presence of OCl⁻ and DCP fluorescence imaging was performed in cell line MDA-MB 231. Briefly, cells were grown in coverslips for 24 hrs. in a 37 °C humidified incubator containing 5% $CO_2$ and then either mock-treated or treated with 10 μM of ligand **TPSA** in the presence or absence of 10 μM working concentration of OCL and 10 μM working concentration DCP separately and incubated for the

5

time period of 15 min and 30 min in dark at 37 ºC. The cells were then washed with 1×PBS three times to remove any unbound TPSA or OCl⁻ or DCP and then they were mounted on a glass slide and detected under fluorescence microscope (Olympus) using DAPI filter .

**Cytotoxicity assay:**

MTT cell proliferation assay[17] was performed to assess the cytotoxic effect of the ligand in **TPSZ** both the cancer cell line MDA-MB-231 and normal cell line WI-38. In brief, cells were first seeded in 96-well plates at a concentration of $1 \times 10^4$ cells per well for 24 h and exposed to the different working concentration of ligand **TPSZ** in Tetrahydrofuran (0 µM, 10 µM, 20 µM, 40 µM, 80 µM, 100 mM) for 24 hrs. After incubation cells were washed with 1×PBS and MTT solution (0.5 mg/ml) were added to each well and incubated for 4 h and the resulting formazan crystals were dissolved in DMSO and the absorbance was measured at 570 nm by using a microplate reader. Cell viability was expressed as a percentage of the control experimental setup.[18]

**4. NMR spectra: ¹H NMR, ¹³C NMR**
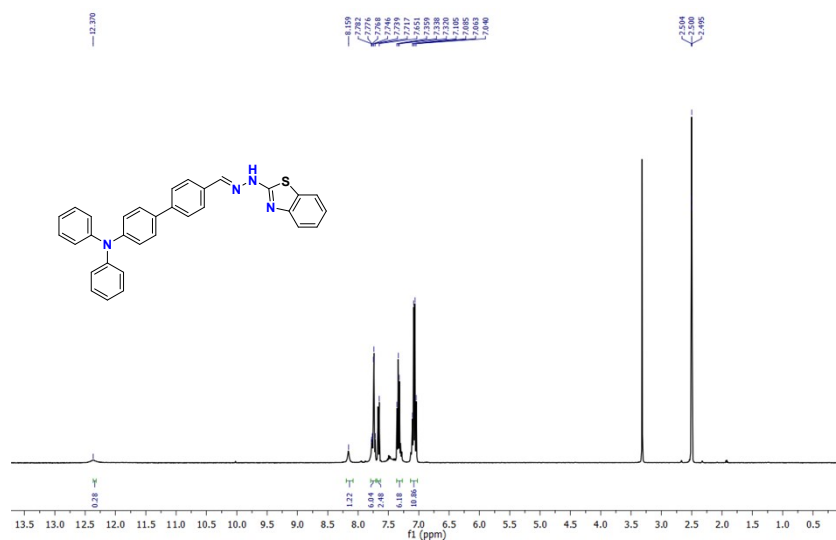


**Figure S2:** ¹H NMR spectrum of **TPSZ** in CD₃CN(400 MHz, 298 K).
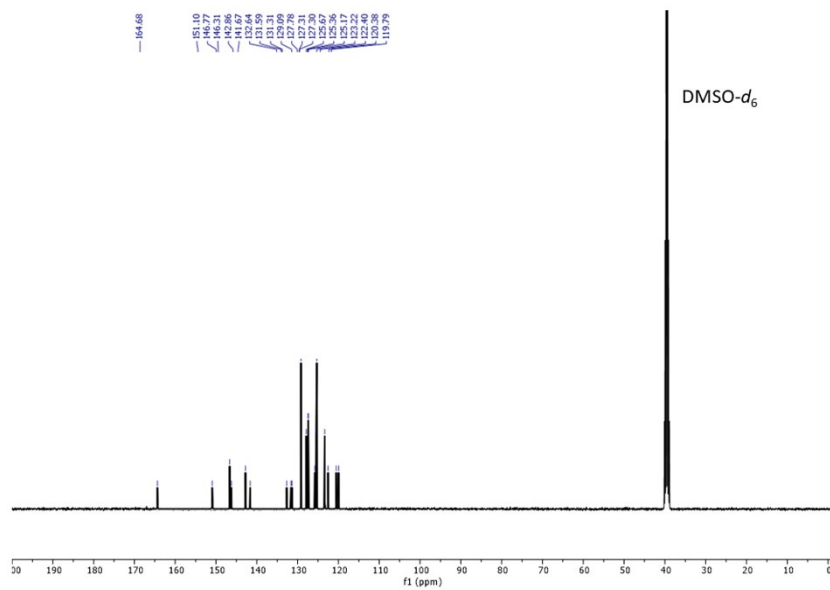
**Figure S3:** $^{13}C$ NMR spectrum of **TPSZ** in CD$_3$CN (100 MHz, 298 K).
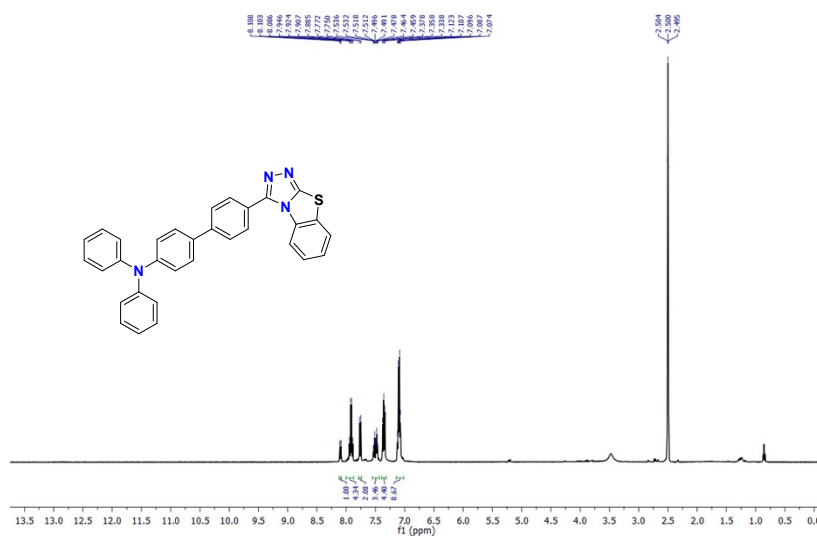


**Figure S4:** $^1H$ NMR spectrum of **TPSZ-OCl** in CD$_3$CN (400 MHz, 298 K).
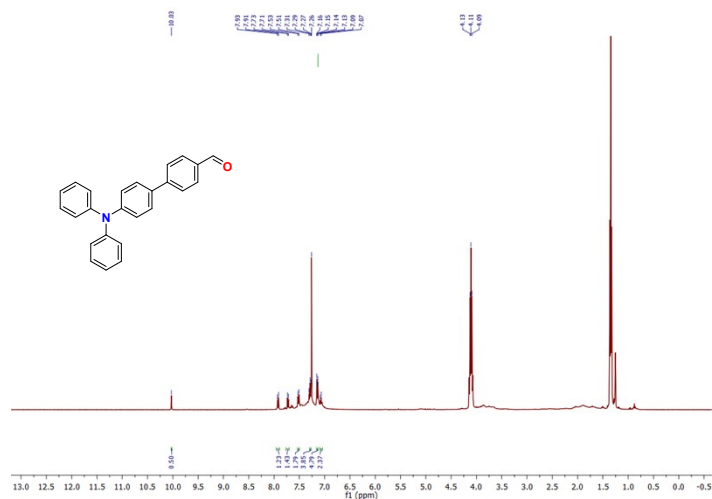
**Figure S5:** ^{1}H NMR spectrum of **TPSZ**-DCP in CD$_3$CN (400 MHz, 298 K).

## 5. ESI-MS Spectra
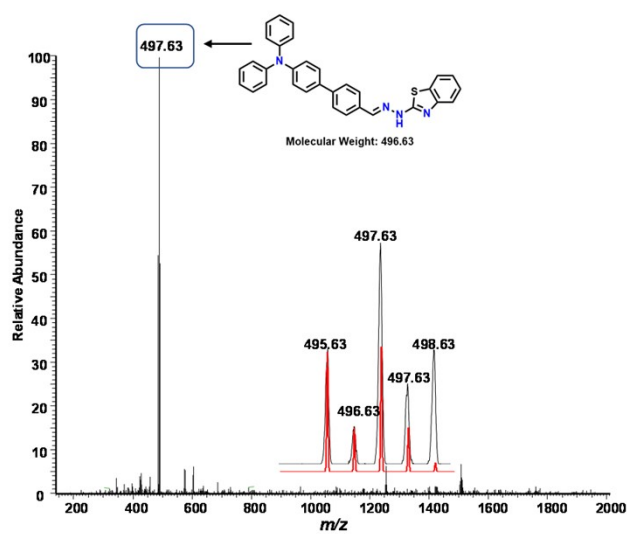


**Figure S6.** ESI-MS of **TPSZ**
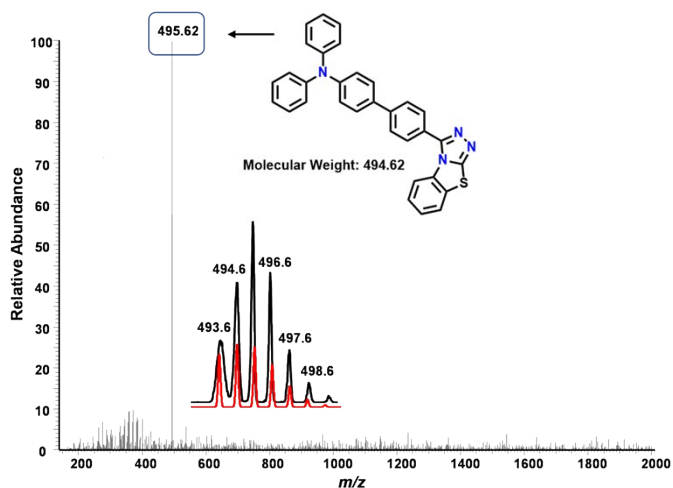
**Figure S7.** ESI-MS of **TPSZ-OCl** after protonation.
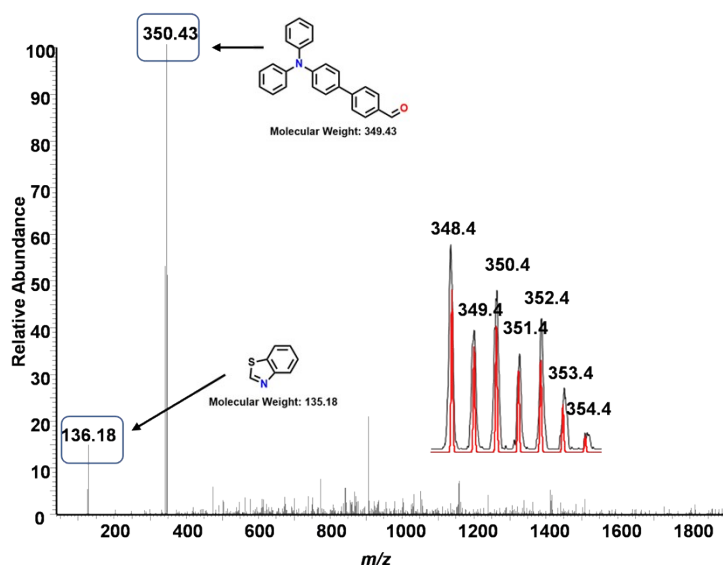


**Figure S8.** ESI-MS of **TPSZ-DCP** after protonation.

## 5. Calculation of Limit of Detection (LOD)

The limit of detection value of the probe **TPSZ** was obtained from a plot of two fluorescence intensity ($I_{505}$ and $I_{460}$) vs. concentration of DCP and OCl⁻ respectively. The S/N ration was determined by the 10 times measurable emission intensity of the **TPSZ** without addition of analytes. and standard deviation of blank measurements was calculated. The LOD value of **TPSZ** for DCP and OCl⁻ was determined by the following equation:

$$LOD = K \times \delta/m$$

Where K= 2 or 3 (We take 3 in this case)

δ is the standard deviation of the blank solution and m is the slope the calibration curve.
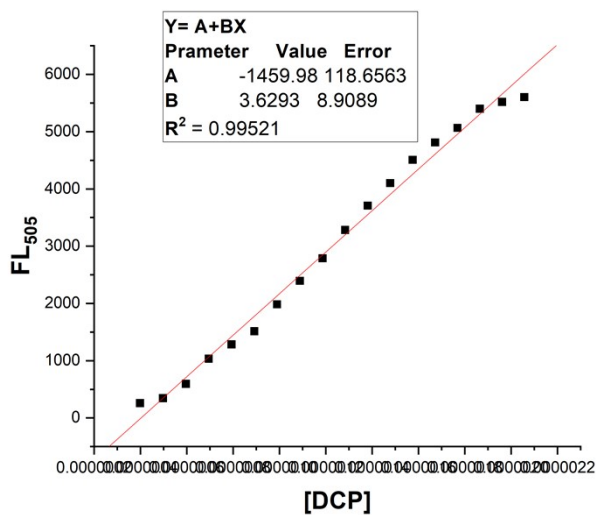


**Figure S9.** Calibration curve of **TPSZ** at ($I_{505}$) depending on DCP concentration
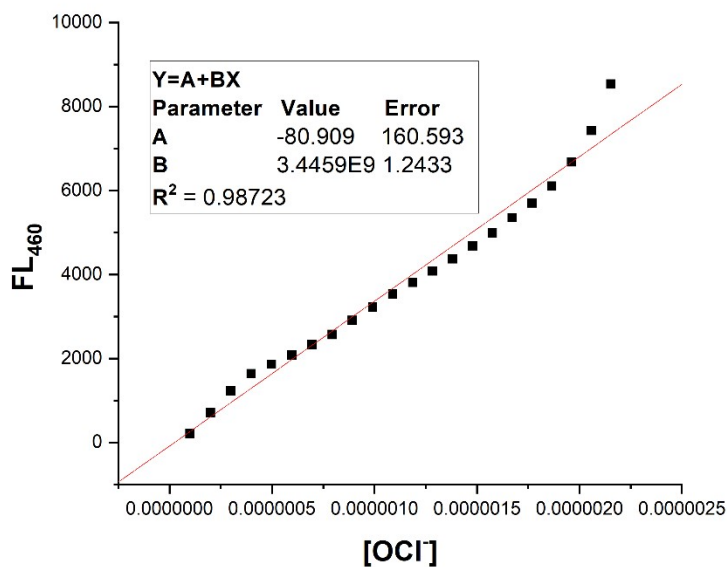


**Figure S10.** Calibration curve of **TPSZ** at ($I_{505}$) depending on OCl⁻ concentration

**References:**

1. B.Huo, M.Du, A.Shen, M. Li, Y. Lai, X.Bai, A. Gong, and Y. Yang, *Anal. Chem.* 2019, **91,** 10979−10983.

2. L.Zeng, H. Zeng, L. Jiang, S. Wang, Ji-T. Hou, and J.Yoon, *Anal. Chem.* 2019, **91**, 12070−12076.

3. S. Goswami, S. Das and K.Aich, *RSC Adv.,* 2015, **5**, 28996.

4. U. N. Guria, K. Maiti, S. S. Ali, A.Gangopadhyay, S. K.Samanta, K. Roy, Dipankar Mandal, and A.K. Mahapatra, *ChemistrySelect.* 2020, **5**, 3770 –3777.

5. K. Aich, S. Das, S. Gharami, L. Patra and T. K. Mondal, *New J. Chem.,* 2017, **41**, 12562.

6. S. Goswami, A.Manna and S. Paul, *RSC Adv.,* 2014, **4**, 21984

7. T.Qin, Y. Huang, K. Zhu, J. Wang, C. Pan, B.Liu, L.Wang, *Analytica Chimica Acta.* 2019, **1076,** 125-130

8. S. S. Ali, A. Gangopadhyay, A. K.r Pramanik, U. N.Guria, S. K. Samanta, A. K.Mahapatra, *Dyes and Pigments.* 2019, **170**, 107585.

9.X.Hua, H. Zengb, T. Chenb , H.-Q. Yuanc , L.Zengb, G.-M. Baoc, *Sensors & Actuators: B. Chemical.* 2020, **319,** 128282.

10. Y.Jiang , S. Zhang, B. Wang, T. Qian, C.Jin, , S. Wu, J. Shen, *Tetrahedron.* 2018,**74**,5733-5738.

11. X.-x. Xu, Y. Qian, *Spectrochimica Acta Part A: Molecular and Biomolecular Spectroscopy.* 2017,**183,**356–361.

12. X.He, C. Xu, W. Xiong, Y.Qian, J. Fan, F. Ding, H.Deng, H.Chen and J. Shen, *Analyst,* 2020, **145**, 29.

13. W.C. Chen, P.Venkatesan, S.-P. Wu, *Analytica Chimica Acta.* 2015, **882,** 68-75.

14. X.-H. Zhou, Y.-R. Jiang, X.-J. Zhao, D. Guo, *Talanta.* 2016,**160**, 470–474.

15. M. Ren, J. Nie, B.Deng, K. Zhou, J.-Y. Wang and W. Lin, *New J. Chem.,* 2017, **41**, 5259.

16. H.Yua, Y. Wuc , Y. Hua , X.Gaoa , Q.Lianga , J. Xua, S.Shaoa, *Talanta.* 2017,**165**, 625–631.

[17].P. R.Twentyman, M. Luscombe, *Br. J. Cancer.* 1987, **56**, 279–285.

[18]. M.Mandal, D. Sain, Md. M. Islam, D. Banik, M. Periyasamy, S. Mandal, A. K. Mahapatra and A. Kar, *Anal.Methods.* 2021,**13**, 3922.